LAWRENCE
LIVERMORE
NATIONAL
LABORATORY

LLNL-CONF-412562

STATUS OF THE DIELECTRIC WALL ACCELERATOR

G. J. Caporaso, Y-J. Chen, S. Sampayan, G. Akana, R. Anaya, D. Blackfield, J. Carroll, E. Cook, S. Falabella, G. Guethlein, J. Harris, S. Hawkins, B. Hickman, C. Holmes, A. Horner, S. Nelson, A. Paul, D. Pearson, B. Poole, R. Richardson, D. Sanders, K. Selenes, J. Sullivan, L. Wang, J. Watson, J. Weir

April 28, 2009

Particle Accelerator Conference
Vancouver, Canada
May 4, 2009 through May 8, 2009

Disclaimer

STATUS OF THE DIELECTRIC WALL ACCELERATOR*,+

George J. Caporaso#, Y-J. Chen, S. Sampayan, G. Akana, R. Anaya, D. Blackfield, J. Carroll, E. Cook, S. Falabella, G. Guethlein, J. Harris, S. Hawkins, B. Hickman, C. Holmes, A. Horner, S. Nelson, A. Paul, D. Pearson[a], B. Poole, R. Richardson, D. Sanders, K. Selenes[c], J. Sullivan, L. Wang, J. Watson and J. Weir[b]

Lawrence Livermore National Laboratory, Livermore CA 94551
[a]Tomotherapy, Inc., Madison WI 53717
[b]Compact Particle Acceleration Corporation, Madison WI 53717
[c]TPL Corporation, Albuquerque, NM 87109

Abstract

The dielectric wall accelerator (DWA) system being developed at the Lawrence Livermore National Laboratory (LLNL) uses fast switched high voltage transmission lines to generate pulsed electric fields on the inside of a high gradient insulating (HGI) acceleration tube. High electric field gradients are achieved by the use of alternating insulators and conductors and short pulse times. The system is capable of accelerating any charge to mass ratio particle. Applications of high gradient proton and electron versions of this accelerator will be discussed.

The status of the developmental new technologies that make the compact system possible will be reviewed. These include, high gradient vacuum insulators, solid dielectric materials, photoconductive switches and compact proton sources.

INTRODUCTION

This paper focuses on one concept that represents an extreme variant of a high gradient accelerator that has been under development as a compact flash x-ray radiography source [1]. The system is called the Dielectric Wall Accelerator (DWA) and employs a variety of advanced technologies to achieve high gradient. Progress towards the development of this concept is proceeding on several fronts. The key technologies for any DWA are high gradient vacuum insulators [2], high bulk breakdown strength dielectrics for pulse forming lines, and closing switches compatible with operation at high gradient. For protons, we describe a very compact source capable of generating substantial currents. In addition, some new accelerator architectures will be described.

* Multiple patents pending.

+ This work was performed under the auspices of the U.S. Department of Energy by Lawrence Livermore National Laboratory under Contract DE-AC52-07NA27344.

caporaso1@llnl.gov

DWA FOR SHORT PULSES

DWA technology originated with a desire for more compact flash x-ray radiography sources [1]. A number of these machines are induction linacs and have average accelerating gradients in the range of 0.3 – 0.5 MeV/m with pulses that are tens of nanoseconds long. Because of the characteristics of vacuum surface insulators that make up the dielectric wall, the highest gradients are attainable for the shortest duration pulses. That fact suggested the architecture illustrated in Figure 1.

The beam tube of the accelerator is an HGI which is capable of supporting a substantial tangential electric field. If the spatial extent of this electric field satisfies a simple constraint derived in [1] then the on-axis field is comparable to the field along the wall. For non-relativistic particles the constraint is basically that the axial extent of the field is greater than about 1.5 x the diameter of the tube.

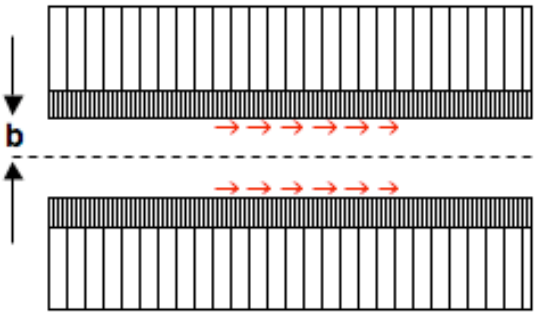

Figure 1: Schematic of a short pulse DWA. The beam tube of radius b is a high gradient insulator [2]. The vertical lines indicate the conductors of transmission lines that supply pulsed voltages across the HGI. The arrows denote the tangential electric field along the insulator surface that fills the volume of the tube to provide acceleration to a co-moving bunch. The voltages are supplied by individual pulse generating lines that are timed to produce a virtual traveling wave of excitation along the tube.

The pulsed voltages that are applied across the dielectric wall in Figure 1 are generated by "Blumlein" type structures with closing switches. The timing of the switches determines the propagation speed of the virtual traveling wave of excitation along the wall.

PHOTOCONDUCTIVE SWITCH DEVELOPMENT

In order to generate pulses in the generic Blumlein structures a good closing switch is required. The ideal switch should have fast rise-time, low "on" resistance and free from latch-up or avalanche at very high electric field stresses. Wide bandgap materials illuminated with below bandgap laser light offer this possibility. The below bandgap light is able to propagate a cm or two through the side of a wafer and illuminate the entire wafer volume, permitting the placement of electrodes on opposite sides of the wafer to take advantage of the high bulk breakdown strength of these materials [3]. Both SiC and GaN wafers have been used. SiC has been used with both 1064 and 532 nm radiation. It is important to note that these devices are actually *light controlled resistors*.

Early tests used materials with "micropipe" defects in the wafers which significantly compromised the bulk breakdown strength of switches. Newly available material is free from these defects.

Figure 2: Three failed SiC photoconductive switches that were soldered into Blumlein-like pulse generating lines. These switches are 1 cm x 1cm x 1mm thick with circular electrodes on top and bottom. The switches failed when charged to in excess of 30 kV for an average field stress of > 30 MV/m. Because of the geometry there is a x 10 field enhancement at the edges of the electrode that pushes the field to ≈ 350 MV/m, which is in excess of the bulk breakdown strength of the material. Each of the failures occurred at an electrode edge where the field stress was computed to be a maximum. Developing an enhancement-free, integrated switch package is the near term goal of our efforts.

The computed electric field stress for the configuration used in the experiments is shown in Figure 3 along with a schematic of the switch, electrodes, solder pads and oil. The maximum field strength, well in excess of the intrinsic bulk breakdown strength of SiC, corresponds to the breakdown sites in the switches shown in Figure 2.

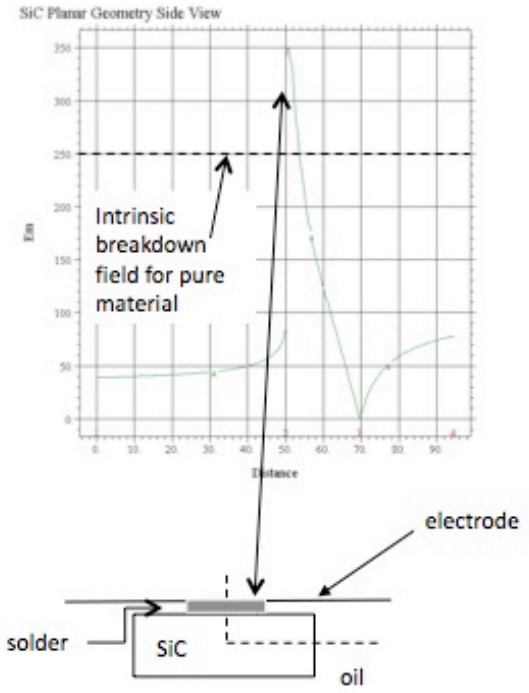

Figure 3: SiC photoconductive switch geometry and field stress distribution along the top surface of the wafer.

CAST DIELECTRIC MATERIAL

Ultimately we would like to use a cast solid dielectric material in the pulse forming lines to simplify the fabrication process and to reduce the cost. For high gradient applications pulses on the order of a few nanoseconds are required. We have been working with materials in which nano-particles of high dielectric constant material are suspended in various base substances such as epoxy, so as to permit adjustment of the relative permeability of the composite. For low concentrations of the nano-particles, the bulk breakdown strength of the material under DC and pulsed conditions in small samples is > 400 MV/m. In recent tests we have measured the breakdown level for larger transmission line structures that are relevant for the accelerator. A test sample of the material is shown in Figure 4.

Figure 4: A test sample of the cast dielectric material in a transmission line configuration. These samples consisted of the base material only (epoxy) with no nano-particles. The dimensions of the sample are 4 cm x 22 cm. The separation between the two, parallel electrodes is 0.8 mm. The electrodes are 0.127 mm thick and 1 cm wide with rolled edges and are embedded within the epoxy. This sample failed along the edge of an electrode at a pulsed voltage of 140 kV for an average field stress between the electrodes of 170 MV/m.

FIRST ARTICLE SYSTEM TEST (F.A.S.T.)

F.A.S.T. stands for First Article System Test, a small, stacked Blumlein accelerator consisting of a small number of solid dielectric pulse generators, photoconductive switches and a high gradient insulator. The system is designed as an integrated test of all of the relevant components of an accelerator. F.A.S.T. is built with a relatively small number of lines so that the system can be easily disassembled to repair failed components at a modest cost. All the switches are illuminated with an expanded laser beam producing simultaneous firing of all the pulse generating lines. While it was initially anticipated that the FR-4 solid dielectric in the pulse generating lines would be the electrical weak point, it turned out that some switches failed via bulk breakdown. Inspection revealed numerous structural defects (known as "micropipes") that are strongly suspected to have compromised the bulk breakdown strength of the wafers. Our first SiC wafers, from a different supplier, were free of these defects and exhibited bulk breakdown strength close to the expected value for pure SiC (≈ 250 MV/m). We have since obtained new SiC from another source that appears to be free of these structural defects.

The pulse generating lines were coupled directly into the HGI. Initial beam tests employed F.A.S.T. as a diode by using a flashboard cathode to provide a source of electrons. A wire mesh was placed on the anode side of the HGI. Tens of Amps were extracted. Since the impedance of the Blumleins was about 40 Ohms, the electron beam constituted a negligible load on the lines. As a consequence, the output voltage across the HGI would ring for several cycles. With each cycle electrons would be extracted from the source when the voltage was of the proper polarity.

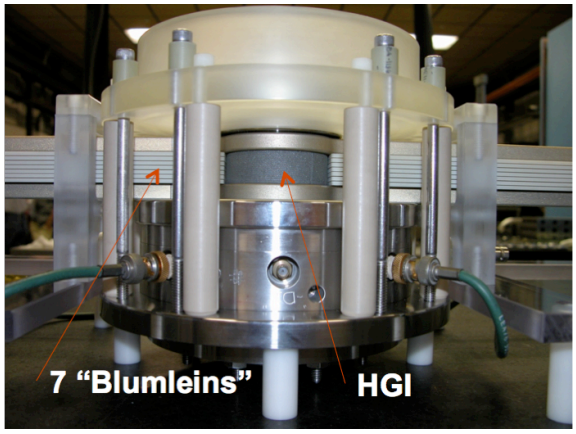

Figure 5: F.A.S.T. set up to accelerate electrons from a flashboard cathode. A 2.5 cm high HGI with a 4 cm bore is the wall of a diode. Two stacks of 7 "Blumleins" are shown feeding the HGI on either side. In some experiments, the diode was operated with a single stack. A sensitive beam current monitor is mounted below the HGI.

PROTON INJECTOR AND SOURCE

In order to accelerate protons through F.A.S.T. they must move fast enough to cross the HGI during the 3 ns accelerating pulse. This requires the protons have at least 200 keV before they enter F.A.S.T. This energy is provided by the injector shown in Figure 6. The output of the induction cells is summed along an internal stalk and appears across a gap approximately 3 cm wide. The cells are driven by cable Blumleins. The injector has been operated at up to almost 300 kV.

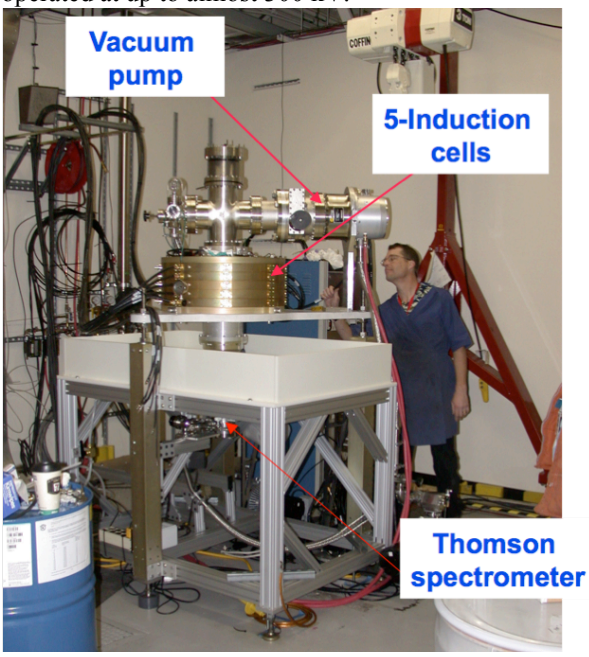

Figure 6: Proton injector built from 5, 20 ns induction cells arranged in an inductive adder configuration to provide a voltage across a 3 cm gap. The source of Figure 7 and a series of gridded, pulsed electrodes, is used to generate the proton beam. F.A.S.T. sits in the white oil tank just below the injector.

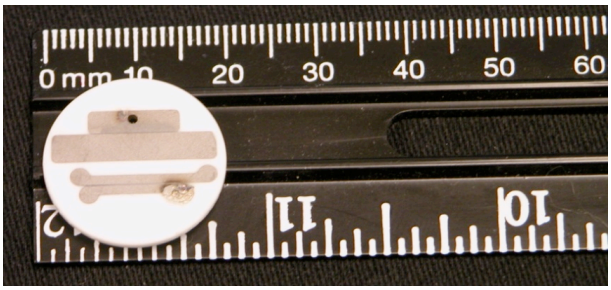

Figure 7: A spark discharge source provides the protons through a small aperture. Titanium electrodes are exposed to a hydrogen atmosphere to absorb the gas (two different sources are shown mounted on an alumina substrate). In operation, a pulsed high voltage is applied to cause a spark between adjacent electrodes that liberates hydrogen gas and forms a plasma. A series of powered grids is used to extract ions, suppress electrons and to gate the output pulse.

ARCHITECTURE ISSUES

Stacked Blumleins, even in a stripline configuration, are relatively low impedance structures. However, the currents flowing in these lines produce magnetic fields that close in adjacent lines. These fields induce currents in those lines that act to reduce the voltage output and distort the waveshape. The use of radial lines will eliminate these parasitic couplings but the impedance of these structures is exceedingly low, requiring massive currents to produce high gradient.

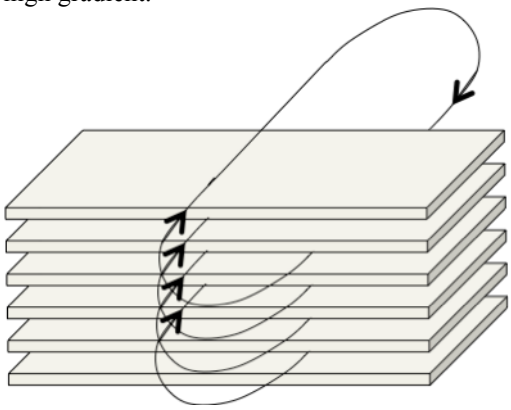

Figure 8: Stacked Blumleins are subject to a parasitic coupling that induces currents in adjacent lines. These currents reduce the overall output voltage and distort the waveshape.

INDUCTION CONCENTRATOR

A possible solution to the problem of parasitic coupling and the relatively low impedance of the stacked Blumlein structures is to use a structure constructed inside of conventional induction cells.

Consider the structure shown in Figure 9. It is an inductive voltage adder in which the voltages of individual induction cells are made to appear across a small gap.

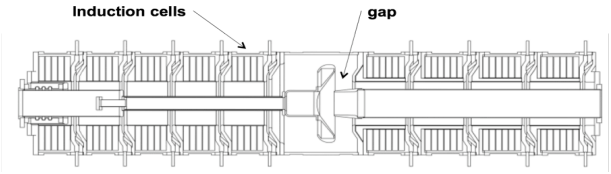

Figure 9. A typical electron injector made from induction cells. The sum of the voltage appears across the gap in the interior adder stalk.

If we could move the injector at the same speed as a particle crossing the gap, it would be continuously accelerated. A possible method for achieving this would be to replace the adder stalk with a tube whose conductivity could be quickly adjusted. Figure 10 shows a technique to do this by using photoconductive switches placed along an insulating tube.

The simplified transmission line circuit for this structure is shown in Figure 11.

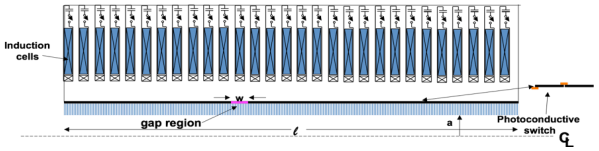

Figure 10. Inductive voltage adder with a stalk lined with photoconductive switches.

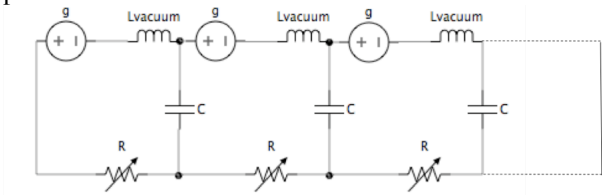

Figure 11. Simplified equivalent circuit for the structure of Figure 10. The distributed voltage sources represent the induction cells, the inductors and capacitors represent the distributed parameters of the coaxial region between the stalk and induction cells. The variable resistors represent the photoconductive switches. By illuminating these in sequence we can create a moving *virtual gap* that can provide continuous acceleration across the entire tube.

The transmission line equations for the voltage V and current i are

$$\frac{\partial V}{\partial x} = -g(x,t) - L\frac{\partial i}{\partial t} - R(x,t)i, \quad \frac{\partial i}{\partial x} = -C\frac{\partial V}{\partial t} \quad (1)$$

where g is the source voltage per unit length supplied by the induction cells, L is the inductance per unit length of coaxial region between the inner stalk and the inner surface of the induction cells, R is the resistance per unit length of the switches (which is controlled by varying the illumination level) and C is the shunt capacitance per unit length. In addition, the electric field along the stalk, which is the accelerating field, is simply given by

$$E_a = -R(x,t)i \; . \quad (2)$$

To analyze this circuit it is convenient to define dimensionless independent and dependent variables.

$$\eta \equiv \frac{R_o t}{L}, \quad \xi \equiv \frac{x}{w}, \quad \psi \equiv \frac{R_o i}{g_o}, \quad \Omega \equiv \frac{V}{g_o w} \quad (3)$$

which are respectively, dimensionless time, distance, current and line voltage. Here, w is the axial extent of the virtual gap, R_o is the minimum resistance per unit length of the switches and g_o is the maximum voltage per unit length supplied by the cells (source function). In addition, the resistance of the photoconductive switches and the source voltage per unit length are given by

$$R(\xi,\eta) = R_o f(\xi,\eta), \quad g(\xi,\eta) = g_o \hat{g}(\xi,\eta). \quad (4)$$

We now wish to look for a traveling wave of excitation along the line. That is, we put

$$f(\xi,\eta) = f\left(\frac{Lu}{R_o w}\eta - \xi\right) \quad (5)$$

where u is the speed of the virtual gap.

Consider a system that is very long so that we may neglect the boundary conditions of the system and seek a traveling wave similarity formulation of the problem. That is, we seek a solution in which all dependent variables are functions of the dimensionless quantity

$$\sigma \equiv \frac{Lu}{R_o w}\eta - \xi. \tag{6}$$

With equations (3) through (6) the system of equations (1) can be reduced to

$$\frac{\left(1-LCu^2\right)}{wR_oCu}\frac{\partial\psi}{\partial\sigma} - f(\sigma)\psi = 1 \tag{7}$$

with

$$E_a = -g_o f(\sigma)\psi(\sigma) \tag{8}$$

where we have taken the source function to be one.

Examination of equation (7) reveals that there are two distinct regimes: $LCu^2<1$ ("subluminal") and $LCu^2>1$ ("superluminal"). This terminology arises from the fact that 1/LC is the square of the speed of an electromagnetic wave along the coaxial system described by equations (1).

If we assume that E_a is a constant over the gap we may use equation (7) to solve for the dimensionless current. Using equation (8) then specifies the function f. Analyses of these two cases reveals that the maximum gain in the strongly subluminal regime is given by

$$\frac{E_a}{g_o} \le 1 + \frac{1}{wR_oCu} \tag{9}$$

while the maximum gain in the strongly superluminal regime is given by

$$\frac{E_a}{g_o} \le 1 + \frac{Lu}{R_o w}. \tag{10}$$

To increase the gain as a particle is accelerated, transition to the superluminal regime is desirable. One way to accomplish this is to load the coaxial system of Figure 10 with toroidal magnetic cores placed beween the stalk and induction cells to increase L. The circuit model is identical with a larger L.

There is a topological dual to the circuit in Figure 11 in which the resistance and inductance are interchanged. In this case the inductance can be produced by a helix along the dielectric beam tube. The switches can be folded inside the induction cells where they are used to power the cells by connecting a capacitor bank across the cell gaps. This arrangement is shown in Figure 12.

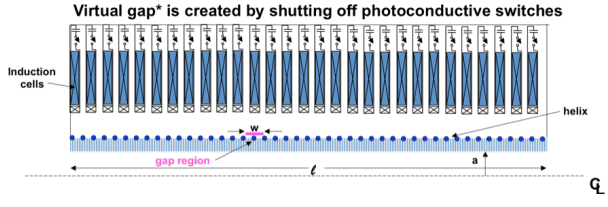

Figure 12. Topological dual to the circuit of Figure 11 in which L and R are interchanged. L is now provided by a helical winding along the dielectric beam tube.

We must now consider the effective resistance of the cores in the induction cells that appears in parallel with the variable switch resistance and source function.

A similarity solution for this case is shown in Figure 13. for the case in which f is exponentially growing (corresponding to carrier recombination after laser light is removed from the switches). Compare this against a numerical solution of the full equations for a 2 meter section (with boundary conditions) as shown in Figure 14.

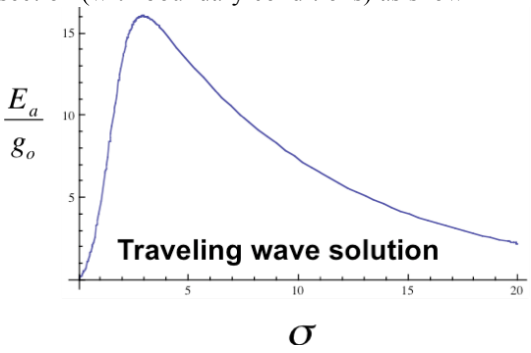

Figure 13. Similarity solution of the circuit corresponding to Figure 12 with core resistance in parallel with the source and switch.

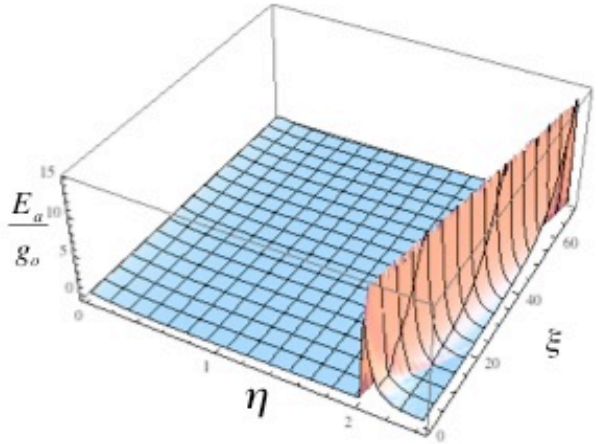

Figure 14. Full numerical solution for a finite line with a wave launched at eta = 2 for the same case as Figure 13.

CONCLUSION

We have described the DWA component development status, discussed the proton injector and source for proton therapy development and have described a new accelerator architecture, the induction concentrator.

REFERENCES

[1] G. Caporaso, et. a., "High Gradient Induction Accelerator", Proc. 2007 U.S. Part. Acc. Conf., TUYC02.

[2] S. Sampayan, et. al., IEEE Trans. Diel. and Elec. Ins. 7 (3) pg. 334 (2000).

[3] J. Sullivan and J. Stanley, "6H-SiC Photoconductive Switches Triggered Below Bandgap Wavelengths", in Proc. 27 Int. Power Modulator Symposium and 2006 High Voltage Workshop, Washington, D.C. 2006.